

Blockage Effect on the Drag of an Axisymmetric Underwater Body in Towing Tank Tests

Yieng Teen Huong, Australian Maritime College, yiengteen.huong@utas.edu.au

Zhi Quan Leong, Australian Maritime College, zhi.leong@utas.edu.au

Jonathan Duffy, Australian Maritime College, j.duffy@utas.edu.au

Alexander Conway, DST Group, Australian Maritime College,

Alexander.Conway@dst.defence.gov.au

Dev Ranmuthugala, DST Group, dev.ranmuthugala2@dst.defence.gov.au

Martin Renilson, Australian Maritime College, martin@renilson-marine.com

ABSTRACT

Towing tanks are regularly used to measure the drag of underwater vehicles. Depending on the ratio of cross-sectional area between the vehicle model and the towing tank, blockage effects can be present that can significantly impact the accuracy of the measurement. To address blockage effects, blockage correctors have been developed over the years for surface ship experiments in towing tanks, and bluff bodies and aircraft in wind tunnels. However, the accuracy of these blockage corrector formulae is yet to be established for underwater vehicles tested in water channels. This paper investigates the blockage effects for an axisymmetric underwater vehicle model tested within a water channel with different blockage parameter ratios using Computational Fluid Dynamics (CFD).

Existing captive-model experimental datasets are used to validate the CFD model. The validated numerical model is then extended to investigate the relationship between the blockage parameter ratio, the velocity of the model, and its predicted drag. Results show that the blockage effect acting on the deeply submerged model is independent of Reynolds number for the speed range considered and the percentage increase in the drag coefficient is linearly proportional to the blockage parameter ratio. CFD predictions are then compared with ITTC and Wind Tunnel blockage correction formulae, and the applicability of modified Tamura's and the Wind Tunnel formula in correcting the blockage effect are demonstrated. It is intended to extend these findings to fully-appended underwater vehicle models tested in towing tanks.

NOMENCLATURE

Notation	Description	Units
A_M	Maximum cross-sectional area of axisymmetric model, $\pi D^2/4$	[m ²]
A_T	Cross-sectional area of water channel, $b \times d$	[m ²]
b	Breadth of towing tank	[m]
C_D	Total Drag Coefficient, $D_T/0.5\rho V^2 S$	[-]
d	Water depth of towing tank	[m]
D	Diameter of the axisymmetric model	[m]
D_T	Total Drag force	[N]

Fr_{nd}^2	Depth Froude number, V/\sqrt{gd}	[-]
g	Gravity	[m s ⁻²]
H	Submergence depth from the model's centerline to the free surface	[m]
H^*	Non-dimensional submergence depth, H/D	[-]
L	Overall length of axisymmetric model	[m]
m	Blockage parameter ratio, A_M/A_T	[-]
M	Mach number	[-]
Re	Reynolds number, $\rho VL/\mu$	[-]
S	Wetted surface area	[m ²]
v_m	Model Volume	[m ³]
V	Fluid velocity	[m s ⁻¹]
ρ	Fluid density	[kg m ⁻³]
μ	Kinematic viscosity	[m ² s ⁻¹]
x, y, z	Cartesian coordinates	[m]
y^+	Non-dimensional wall distance	[-]

INTRODUCTION

When a submerged body is tested in a fluid domain surrounded with rigid walls, it experiences blockage effects due to the reduction in the fluid cross sectional area around the body in comparison to the cross sectional area upstream and downstream of the body. The walls restrict the fluid displacement due to the presence of the body, which impacts the surrounding fluid velocity and the wake displacement of the tested body [1]. The blockage effect results in a difference between the measured data and that in open water. Therefore, quantifying the blockage effect or applying a blockage corrector for a submerged underwater vehicle is essential to ensure accurate measurement of its hydrodynamic characteristics.

Blockage effect is strongly correlated with the blockage parameter ratio, m , which is the ratio of the maximum frontal cross-sectional area of the model, A_M , and the cross-sectional area of tank test section, A_T . The work on blockage effect for surface ships tested in towing tanks [2-6] and bluff bodies in wind tunnel [7] has been extensively studied over the years. However, there is limited information in the open literature addressing the blockage effect acting on deeply submerged underwater vehicles tested in towing tanks as well as the formation of relevant blockage corrector formulae. The current ITTC guideline [6] provides the blockage corrector for surface ships tested in towing tanks. However, questions do arise on the applicability of the ITTC and wind tunnel blockage correctors in rectifying the blockage effect acting on the drag force of underwater vehicles obtained from water channels. Hence, the focus of this study is to investigate the applicability of the current surface ship ITTC and wind tunnel methods to the blockage correction for underwater vehicles.

To investigate the influence of blockage effect on the drag of deeply submerged axisymmetric underwater vehicles tested in water channels, RANS-based Computational Fluid Dynamic (CFD) simulations were used to quantify the drag under different domain blockage parameter ratios and Reynolds numbers. The objective was to develop a relevant blockage correction procedure as a function of the blockage parameter ratio, m . The results were also used to

access the applicability of the surface ship based ITTC blockage correction standards to submerged bodies.

TEST PLAN

The geometry used in this study was the bare hull configuration of the generic Joubert model with a length, L , of 1.69 m and a diameter, D , of 0.23 m (see Figure 1). Further details of the geometry can be obtained from [8].



Figure 1: Axisymmetric bare hull Joubert geometry [8]

The model was located at the centre of the cross sectional area of the test section to ensure a symmetrical flow field along its body of revolution profile. A straight line analysis (zero drift and pitch angle) was conducted on the underwater vehicle at speeds ranging between 0.4 m/s to 1.2 m/s, giving a Reynolds number range of 0.6 million to 2 million.

Three tank breadth to depth ($b:d$) ratios (1:1, 2:1 and 3:1) were modelled to investigate the influence of tank confinement effect on the blockage effect acting on the model. Additionally, four blockage parameter ratios, m , were modelled for each tank breadth to depth ratio to study the blockage effect on the total drag coefficient for a fixed tank breadth to depth ratio. Table 1 lists the dimensions of the tank domain and the blockage parameter ratios investigated.

Table 1: Fluid domain size for different breadth to depth ratios and blockage parameter ratios

Tank's breadth (b) to depth (d) ratio	Tank Cross Section, ($b \times d$) (m)	Blockage Parameter ratio, m
1:1	1 x 1	0.0415
	1.2 x 1.2	0.0289
	1.6 x 1.6	0.0162
	10 x 10	0.0004
2:1	2 x 1	0.0207
	2.4 x 1.2	0.0144
	3.2 x 1.6	0.0081
	20 x 10	0.0002
3:1	3 x 1	0.0138
	3.6 x 1.2	0.0096
	4.8 x 1.6	0.0054
	30 x 10	0.0001

SIMULATION SETUP

Simulations were conducted using commercial CFD code, ANSYS Fluent 19.3 to model the fluid flow and the fluid domain used for the investigation as shown in Figure 2. Due to the axisymmetric nature of the underwater vehicle, the domain was split about the x-z plane and only half of it was modelled to optimise the computational effort. Comparison between the half and full model simulations showed a difference in the computed drag coefficient of less than 0.1%. Thus, the former was deemed sufficient for this study. The inlet length from the underwater vehicle's centre of buoyancy (coinciding with the origin of the coordinate system) was two body lengths as recommended by the ITTC CFD verification and validation guideline [9]. The outlet dimension was determined based on the outlet sizing conducted to ensure the chosen outlet distance could resolve the submerged body's wake while avoiding the occurrence of any backflow. The distance to the outlet was sized to be four body lengths from the centre of buoyancy, as a further increase to seven body lengths only resulted in 0.4% change in the drag coefficient.

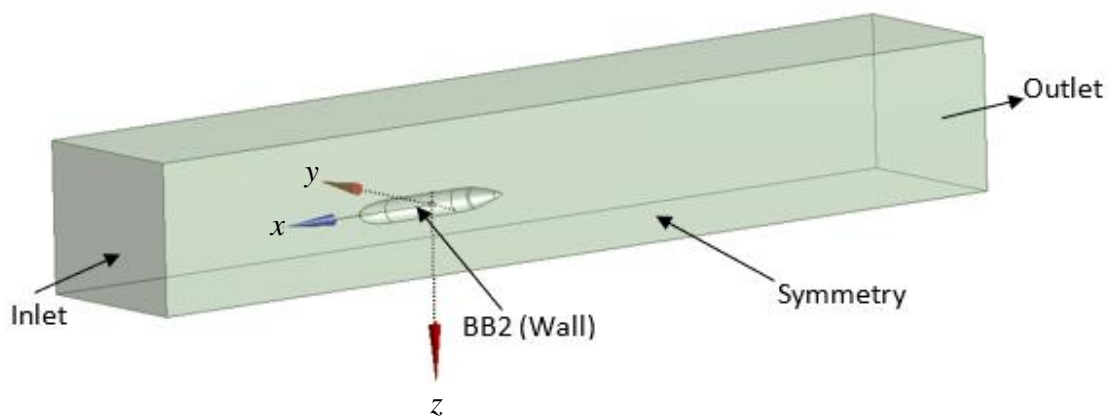


Figure 2: Computational fluid domain with coordinate system.

The computational mesh (Figure 3) was generated utilising ANSYS Fluent Meshing and adopted the Mosaic Meshing Technology [10]. A value of $y^+ = 30$ was used as the first layer prismatic height in combination with the Shear Stress Transport (SST) $k-\omega$ turbulence model. The SST $k-\omega$ model has been proven to model hydrodynamic coefficients of underwater vehicles in the translation motion with low drift and pitch angle accurately and was comparable with previous experimental results [11-15].

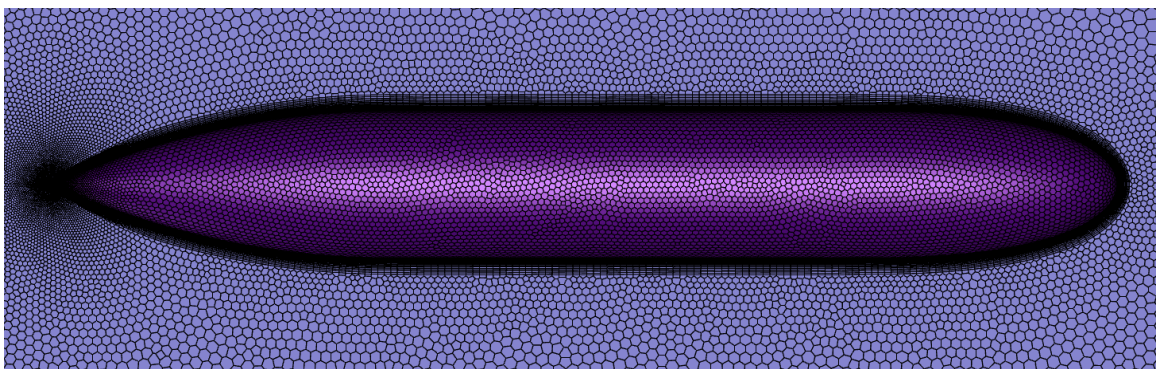


Figure 3: Mesh model of the axisymmetric bare hull Joubert geometry.

The ANSYS Fluent high-resolution scheme (PRESTO for pressure and Third Order MUSCL for momentum, turbulent kinetic energy and specific dissipation rate) was used throughout the simulations. The convergence criteria adapted for the study was that the root mean square value of the global residuals was to be less than $1e-04$, with fluctuations in the predicted drag to be no more than three significant digits over 50 iterations.

VERIFICATION AND VALIDATION

The verification and validation phases of the CFD simulations were carried out against experimental data from the testing of the Joubert axisymmetric hull form in the Australian Maritime College (AMC) towing tank [16]. The computational domain size adapted for the validation study was constructed to replicate the AMC towing tank dimensions (breadth of 3.5 m and a water depth of 1.5 m) to ensure a like-to-like comparison between the numerical and the experimental results. The overall cell count used in the simulation was 1 million, which was deemed sufficient for this study as it provided deviations of less than 0.7% in the predicted drag when compared to the mesh refinement of 5.3 million (see Figure 4).

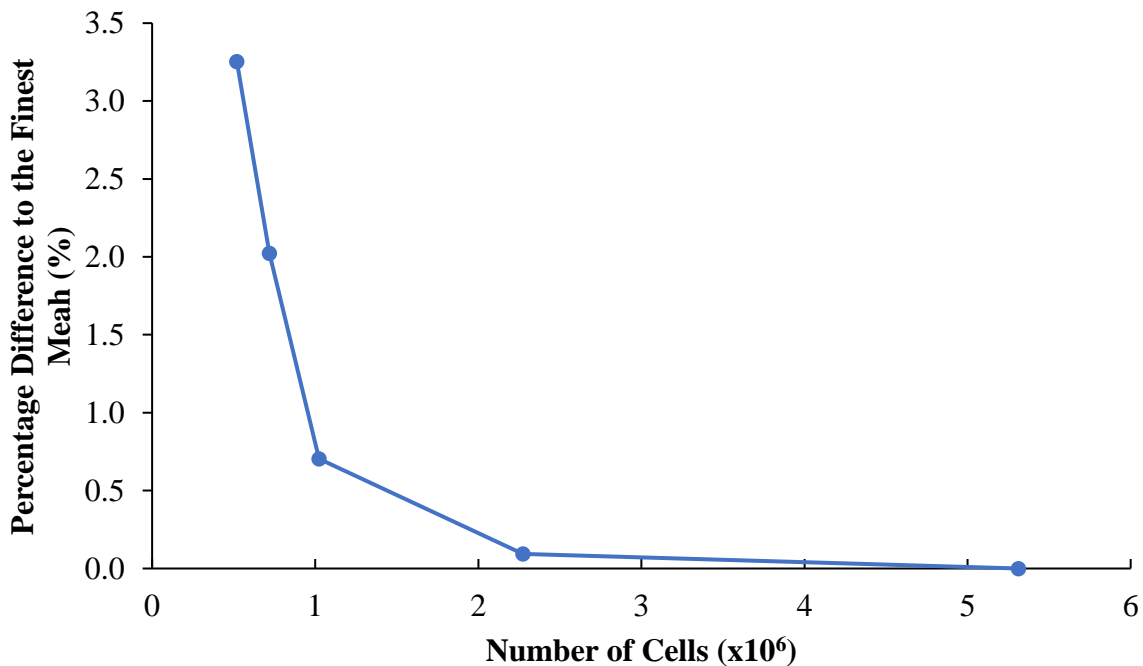


Figure 4: Grid independent study - percentage difference in the predicted drag compared to the finest 7.1 million cell simulation solution.

Validation of the CFD model was carried out using the experimental data obtained by Dawson [16] and is presented in Figure 5. The result shows a discrepancy in magnitude of around 10% between the numerical and experimental drag coefficient at the higher Reynolds Number. Although a higher discrepancy between the numerical and experimental results existed at the higher Reynolds Number, the results were deemed to be sufficiently accurate as most of the numerical results fall within the experimental uncertainty calculated by Dawson [16].

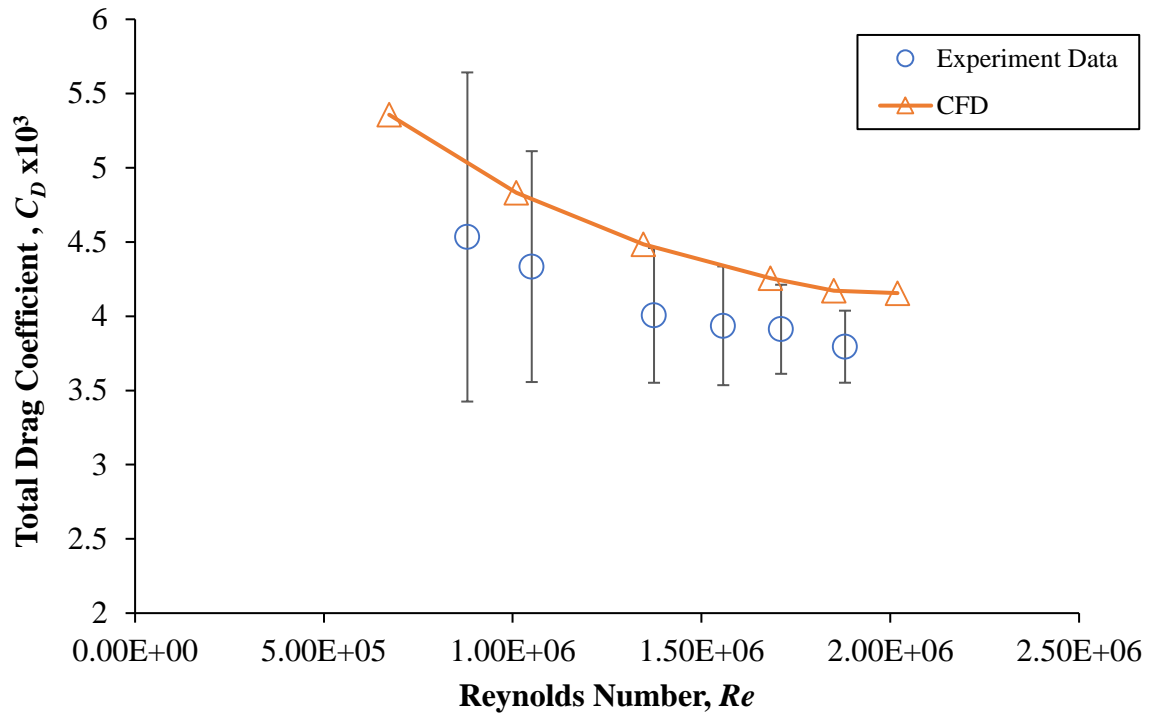


Figure 5: CFD predicted drag coefficients and experimental measurements [16] for the Joubert bare hull geometry in straight line tests, with error bars of maximum 23 % and minimum of 5%.

RESULTS AND DISCUSSION

Figure 6 shows the predicted drag coefficient of the underwater vehicle as a function of Reynolds number for the different blockage parameter ratios (m) and domain ratios ($b:d$). The trends of the predicted results show that an increase in the blockage parameter ratio will increase the drag coefficient acting on the submerged underwater vehicle. The results also show that the drag as a function of Reynolds Number is similar in shape for the different blockage domain ratios examined. The percentage increase in drag coefficient with respect to the largest domain as a function of Reynolds number for different block parameter ratios is given in Figure 7. The constant percentage difference along the Reynolds Number range tested indicating that the blockage effect is independent of Reynolds Number.

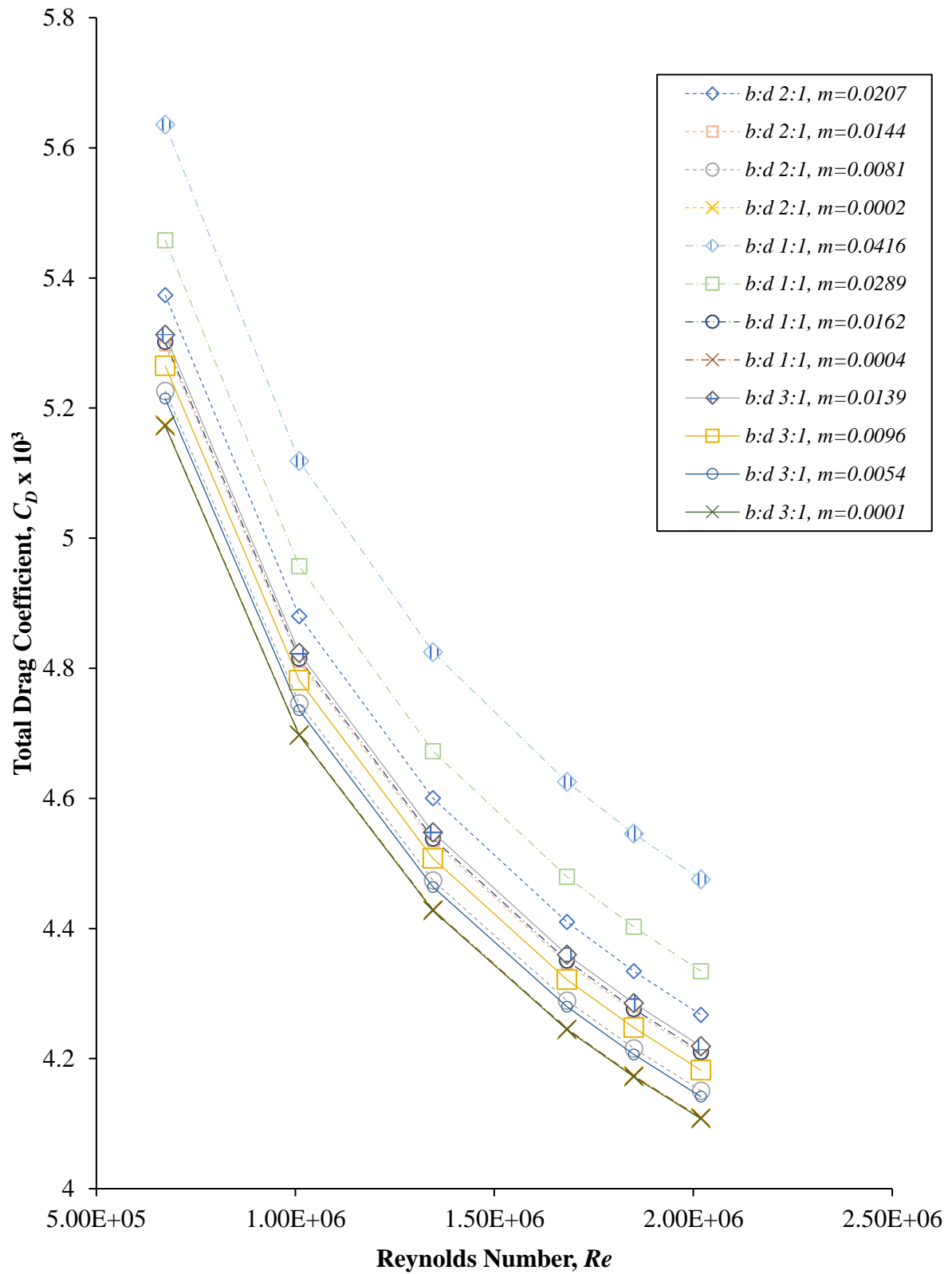


Figure 6: Total drag coefficient, C_D , as a function of Reynolds Number, Re for different domain ratios ($b:d$) and blockage parameter ratios, m .

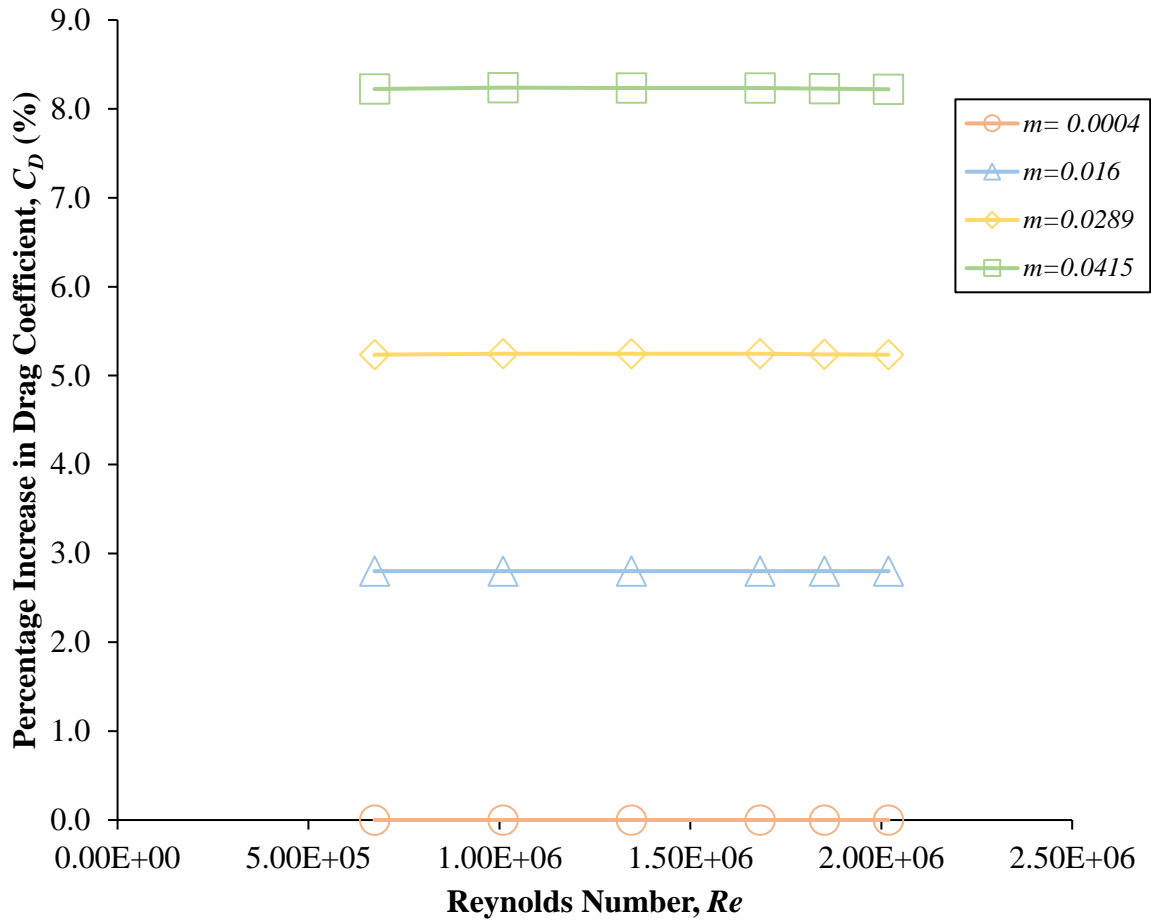


Figure 7: Percentage increase in drag coefficient, C_D , as a function of Reynolds Number, Re , for different blockage parameter ratios, m when compared to the largest blockage parameter ratio, $m=0.0001$

The independency between blockage parameter ratio and Reynolds Number enables the relationship between drag coefficient and the blockage parameter ratio to be quantified. Figure 8 shows the percentage increase in the drag coefficient for the different blockage domain ratios when compared to the largest domain (30 m breadth, 10 m depth, $m = 0.0001$). From Figure 8, it is seen that the percentage increase of the drag coefficient is linearly proportional to the blockage parameter ratio, m , therefore, an estimate of the blockage effect for a deeply submerged body can be obtained using a linear trend line. The increase in total drag coefficient is given by the following proposed empirical equation,

$$\% \text{ increase in } C_D = 186.48 m \quad (1)$$

The proposed blockage effect estimation for a deeply submerged body is shown to fit well with the numerical data, with a coefficient of determination, R^2 of 0.99.

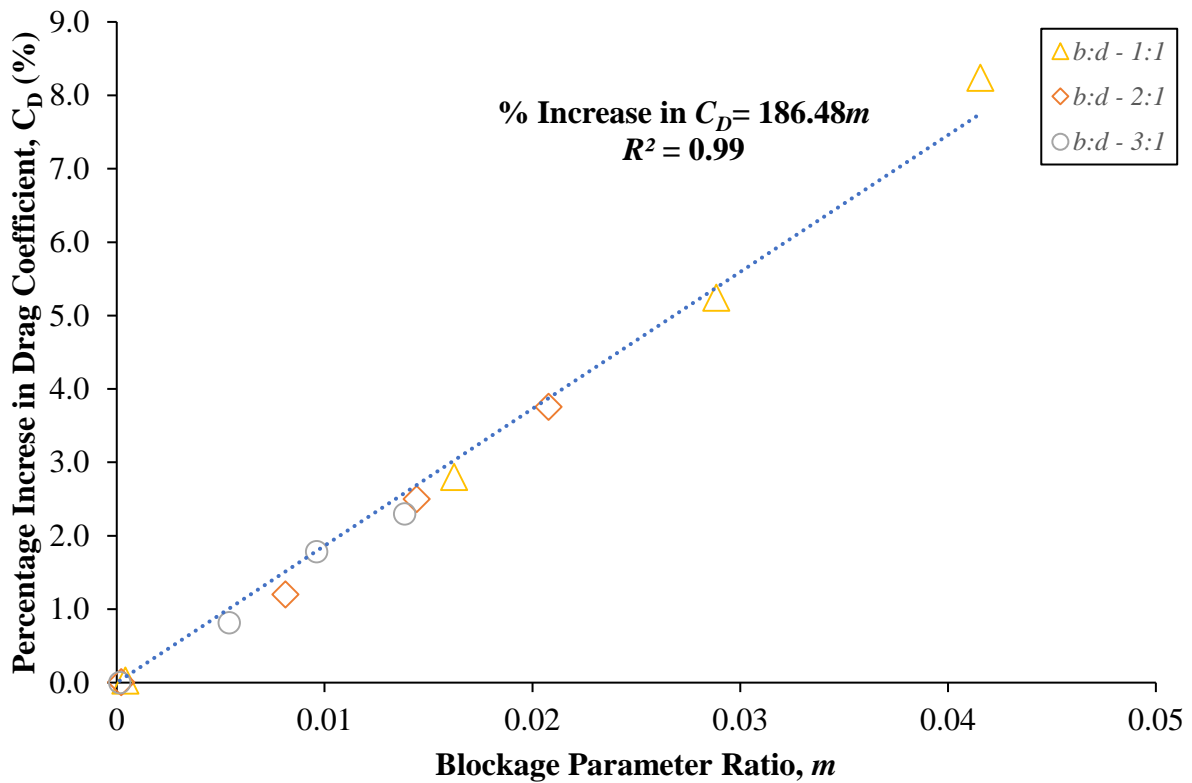


Figure 8: Empirical correction formula for the increase in drag coefficient, C_D , when compared to the largest domain at each blockage parameter ratio, m .

From Figure 8, it is seen that the domain sizing with the breadth to depth ratio of 1:1 displayed an overall higher increase in drag coefficient compared to other domain ratios. The equal distance between the model and the domain walls resulted in a stronger rigid wall interference with the underwater vehicle's flow field. This caused a higher increment in the fluid velocity thus, increasing the predicted drag coefficient in comparison to other domain ratios.

The current study did not include the modelling of the free surface, however, future work will include modelling the towing tank with the free surface at varying submergence depths to quantify the change in the drag coefficient as a function of blockage parameter ratio and submergence.

COMPARISON WITH BLOCKAGE CORRECTORS OF [6] AND [7]

The identification of an appropriate blockage corrector formula for a towing tank test domain is essential in order to accurately predict the drag coefficient of an underwater vehicle in an unrestricted domain. Most studies quantify the influence of blockage in term of velocity increase ratios [2-7]. The effective flow velocity, V , surrounding a submerged underwater vehicle in a water channel is assumed to be the same as the flow speed of the vehicle moving in an unrestricted domain with the velocity of $V+\Delta V$. Using this assumption, the drag force

acting on the vehicle moving in the channel is approximately equal to the drag force acting on the vehicle in an unrestricted domain at the velocity of $V+\Delta V$. This increase in velocity can be obtained using available blockage correction formulae, which include the ITTC [6] and Wind Tunnel [7] blockage correctors.

Among the blockage correctors recommended in the ITTC guideline [6], Tamura's equation is the most applicable equation to correct the blockage effect acting on a deeply submerged underwater vehicle. Tamura's equation was developed based on two fundamental theories, the back flow theory and mean flow theory [3, 4] and is given as,

$$\frac{\Delta V}{V} = 0.67m \left(\frac{L}{b}\right)^{0.75} \frac{1}{(1 - Fr_{nd}^2)} \quad (2)$$

Mean flow theory describes the relationship between the blockage induced velocity increment and the depth Froude number, Fr_{nd}^2 , for a surface ship [2, 3, 5]. However, the Froude effect does not apply for a deeply submerged underwater vehicle, and hence $Fr_{nd}^2 = 0$. This therefore, allows for the isolation of the mean flow based formula presented in the Tamura's equation, yielding the modified Tamura's corrector as,

$$\frac{\Delta V}{V} = 0.67m \left(\frac{L}{b}\right)^{0.75} \quad (3)$$

For the wind tunnel blockage correction, Thom's solid blockage corrector [7] was chosen to correct the velocity of the submerged underwater vehicle's flow field. The equation is given by,

$$\frac{\Delta V}{V} = \frac{k(v_m)}{A_T^{3/2}} \quad (4)$$

where k is 0.96. The performance of each blockage corrector method was compared between the three domain ratios. Figure 9 shows the comparison of the corrected drag coefficient ($Re = 0.6$ million) for different blockage parameter ratio, m , using the ITTC Tamura method [6] (equation (3)), Thom method [7] (equation (4)) and the proposed empirical equation (1) with the numerical predicted drag coefficient at an unrestrained domain, $m=0.0001$.

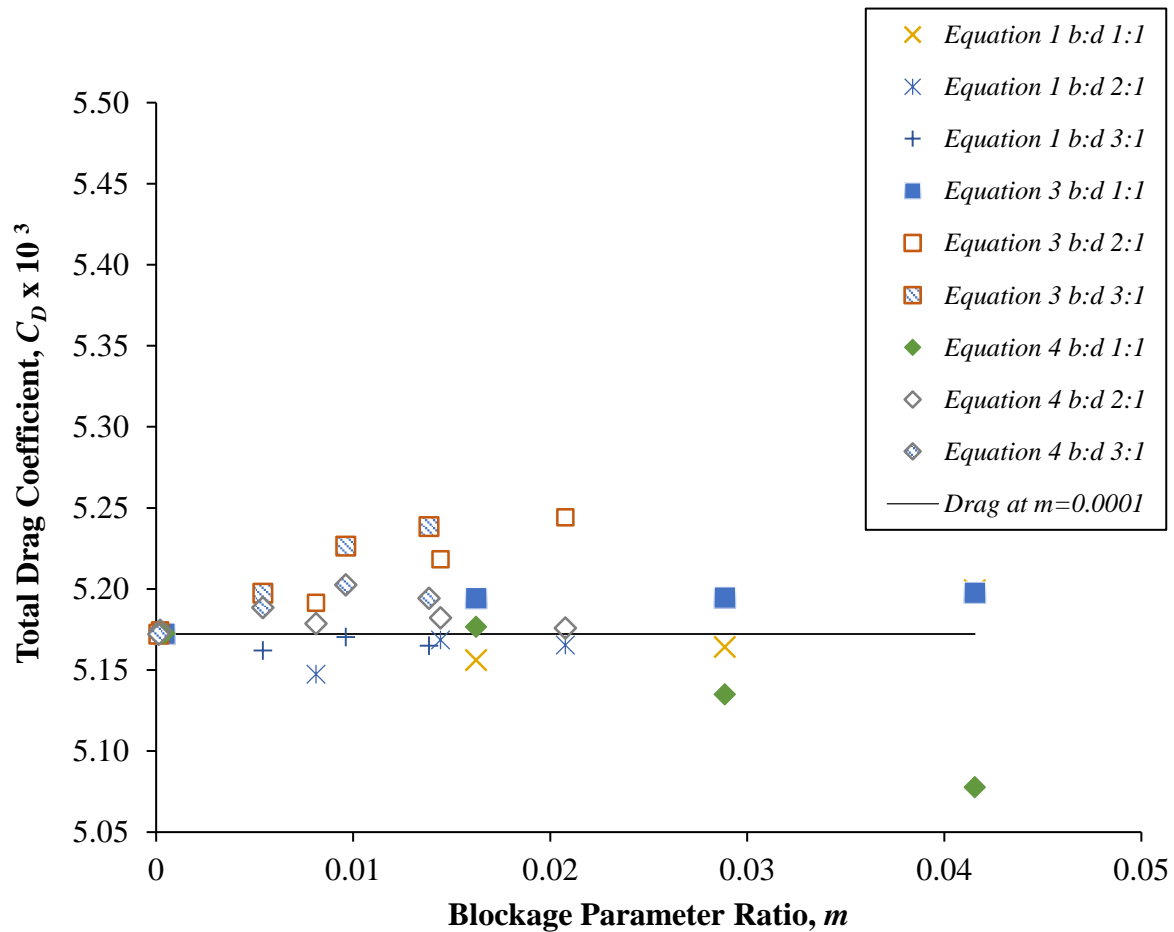


Figure 9: Total drag coefficient, C_D , predicted against blockage parameter ratio, m , at a Reynolds number, Re , of 0.6 million using different correctors.

Although the results show differences between the ITTC Tamura [6], the Thom [7] and the proposed empirical equation when compared to the numerical predicted drag coefficient at unrestricted domain, their discrepancies are within 2%. Thus, all three methods provide reasonable estimations of the blockage corrected drag coefficient based on the blockage parameter ratio for a deeply submerged underwater vehicle model tested in a towing tank for the specified speed range. It is seen that the proposed empirical formula provides the best prediction. However, further studies are required to include the effects of the free surface in predicting the blockage effect when testing underwater vehicles for drag coefficients in towing tanks.

CONCLUDING REMARKS

The paper presented a study conducted to quantify the blockage effect acting on a deeply submerged underwater vehicle tested in a water channel. The investigation utilised CFD simulations to extend the domain size such that the effects of the blockage parameter and the Reynolds Number on the drag coefficient of the underwater vehicle was obtained. Experimental data was utilised to validate the CFD simulation to predict the drag coefficient of the underwater vehicle model tested in the towing tank.

The results indicated that the blockage effect acting on a deeply submerged underwater vehicle model in the towing tank is independent of the Reynolds Number within the range investigated. As the increase in the drag coefficient is directly proportional to the blockage parameter ratio, a linear polynomial was fitted to obtain a proposed formula based correction thus allowing the prediction of the drag coefficient of the vehicle in an unrestricted domain. Comparison with the existing blockage correction methods [6, 7] showed good agreement.

However, as the free surface was not included in the simulations, further work is required to quantify the effect of submergence depth on the drag coefficient blockage corrector when an underwater body is being tested in a towing tank with free surface. Thus, future work includes investigating the influence of Froude number on the blockage effect acting on underwater vehicles tested in towing tanks. This will allow the establishment of a blockage corrector formula for underwater vehicles with variations in blockage parameter and submergence depths. The work will then be extended to fully appended underwater vehicles.

REFERENCES

1. El-Sherbiny, S.e.-S. (1972). *Effect of Wall Confinement on the Aerodynamics of Bluff Bodies*. Doctor of Philosophy, University of British Columbia,
2. Scott, J.,(1970), *On Blockage Correction and Extrapolation to Smooth Ship Resistance*. Transactions of S.N.A.M.E, (7): p. 31.
3. Tamura, K.,(1972), *Study on the Blockage Correction*. Journal of the Society of Naval Architects of Japan. **131**: p. 17-28.
4. Kinya, T.,(1998), *Blockage Correctors and Their Appraisal*. The Bulletin of Nagasaki Institute of Applied Science. **39**(1): p. 1-18.
5. Hughes, G.,(1961), *Tank Boundary Effects on Model Resistance*. Transactions of I.N.A. **103**: p. 421-440.
6. ITTC. (2011). *Testing and Extrapolation Methods- Resistance Resistance Test*, (7.2-02-02-01). International Towing Tank Conference, UK.
7. Rae, W.H. and A. Pope,(1984), *Low-Speed Wind Tunnel Testing*. John Wiley.
8. Joubert, P., (2006), *Some Aspects of Submarine Design. Part 2. Shape of a Submarine 2026*. Defence Science and Technology Organisation Victoria, Australia.
9. ITTC. (2008). *Uncertainty Analysis in CFD Verification and Validation Methodology and Procedures*. (7.5-03-01-01). International Towing Tank Conference, UK.
10. ANSYS, (2018), *ANSYS Fluent Mosaic Technology Automatically Combines Disparate Meshes with Polyhedral Elements for Fast, Accurate Flow Resolution*.
11. Watt, G.D., C.R. Baker, and A.G. Gerber, (2006), *ANSYS CFX-10 RANS normal force predictions for the series model 4621 unappended axisymmetric submarine hull in translation*. Defence Research and Development Canada: Ottawa.
12. Toxopeus, S.,(2008), *Viscous-flow calculations for bare hull DAPRA SUBOFF submarine at incidence* international Ship Building Progress. **55**: p. 227-251.
13. Phillips, A.B., S.R. Turnock, and M. Furlong,(2010), *Influence of Turbulence Closure Models on the Vortical Flow Field around a Submarine Body Undergoing Steady Drift*. Journal of Marine Science and Technology. **15**: p. 201-217.
14. Leong, Z.Q., et al.,(2012), *RANS-based CFD Prediction of the Hydrodynamic Coefficients of DARPA SUBOFF Geometry in Straight-Line and Rotating Arm Manoeuvres*. international Journal of Maritime Engineering. **154**: p. 41-52.

15. Huong, Y.T. (2018). *Numerical Analysis on the Effect of Submergence Depth on the Bare-hull Model Scaled BB2 at AMC Towing Tank.*, University of Tasmania, Launceston, Australia.
16. Dawson, E. (2014). *An Investigation into the Effects of Submergence Depth, Speed and Hull Length-to-Diameter Ratio on the Near-Surface Operation of Conventional Submarines.* Master of Philosophy, Australia Maritime College, Launceston.